ARL-TR-7612 ● FEB 2016

US Army Research Laboratory

Advanced Polymer Network Structures

by Robert Lambeth, Joseph Lenhart, Yelena Sliozberg, and Tim Sirk

NOTICES

Disclaimers

The findings in this report are not to be construed as an official Department of the Army position unless so designated by other authorized documents.

Citation of manufacturer's or trade names does not constitute an official endorsement or approval of the use thereof.

Destroy this report when it is no longer needed. Do not return it to the originator.

ARL-TR-7612 ● FEB 2016

US Army Research Laboratory

Advanced Polymer Network Structures

by Robert Lambeth, Joseph Lenhart, and Tim Sirk
Weapons and Materials Research Directorate, ARL

Yelena Sliozberg
TKC Global, Herndon, VA

REPORT DOCUMENTATION PAGE

Form Approved
OMB No. 0704-0188

1. REPORT DATE *(DD-MM-YYYY)*	2. REPORT TYPE	3. DATES COVERED (From - To)
February 2016	Director's Research Initiative (DRI)	1 October 2012–30 September 2015

4. TITLE AND SUBTITLE
Advanced Polymer Network Structures

5a. CONTRACT NUMBER

5b. GRANT NUMBER

5c. PROGRAM ELEMENT NUMBER

6. AUTHOR(S)
Robert Lambeth, Joseph Lenhart, Yelena Sliozberg, and Tim Sirk

5d. PROJECT NUMBER

5e. TASK NUMBER

5f. WORK UNIT NUMBER

7. PERFORMING ORGANIZATION NAME(S) AND ADDRESS(ES)
US Army Research Laboratory
ATTN: RDRL-WMM-G
Aberdeen Proving Ground, MD 21005-5069

8. PERFORMING ORGANIZATION REPORT NUMBER
ARL-TR-7612

9. SPONSORING/MONITORING AGENCY NAME(S) AND ADDRESS(ES)

10. SPONSOR/MONITOR'S ACRONYM(S)

11. SPONSOR/MONITOR'S REPORT NUMBER(S)

12. DISTRIBUTION/AVAILABILITY STATEMENT
Approved for public release; distribution is unlimited.

13. SUPPLEMENTARY NOTES

14. ABSTRACT
Polymer networks and gels are important classes of materials for defense applications. In an effort to improve the mechanical performance of these materials, we have investigated an approach based on double networks. A new potential method for forming double networks in a single step was identified from coarse-grained molecular dynamics simulations of polymer solvents bearing rigid side chains dissolved in a polymer network. Coarse-grained molecular dynamics simulations also explored the mechanical behavior of traditional double networks and indicated that the elastic modulus and molecular-scale fracture toughness of double networks depend on cross-linked density, the ratio of the highly to loosely cross-linked network, and the network interactions. Several new computation tools were also developed to more accurately describe model polymer networks. Epoxy single network gels were prepared, and it was demonstrated that the length and stiffness of the epoxy precursor can have a profound impact on the final network structure and mechanical behavior. An epoxy-acrylate double network was prepared, and preliminary mechanical evaluation suggested significant improvement in the toughness of the double network over the single network.

15. SUBJECT TERMS
Director's Research Initiative (DRI), polymer networks, polymer gels, molecular dynamics simulations, double networks

16. SECURITY CLASSIFICATION OF:			17. LIMITATION OF ABSTRACT	18. NUMBER OF PAGES	19a. NAME OF RESPONSIBLE PERSON
a. REPORT	b. ABSTRACT	c. THIS PAGE			Robert Lambeth
Unclassified	Unclassified	Unclassified	UU	32	19b. TELEPHONE NUMBER (Include area code) 410-306-0218

Contents

List of Figures

List of Tables

INTENTIONALLY LEFT BLANK.

1. Introduction

The goal of this work was to develop new classes of polymeric networks and gels with enhanced energy dissipation and tunable damping behavior. We focused primarily on the design, synthesis, and characterization of double networks through synergistic interaction between computation and experiment. Double networks are essentially "molecular" composites composed of a rigid primary polymeric network combined with a more flexible secondary network. Analogous to fiber-reinforced composites (rigid fiber in softer polymer), double networks can provide a unique combination of stiffness, toughness, and energy dissipation due to their hybrid nature. These tougher networks and gel will enable a host of Army technologies, including flexible armor, lightweight armor and armor adhesives, composite vehicles, unmanned aerial vehicles, multifunctional composites, robotics, battlefield medical treatments, and prosthetics.

2. Approach

Classic soft materials, such as hydrogels, suffer from poor mechanical performance. This has been overcome, in part, by preparing double network hydrogels. Double networks are an emerging class of cross-linked polymers that offer the potential to revolutionize the polymers community. Current state-of-the-art rubbers reach tensile strengths near 30 MPa and elongation at breakup to 800%.[1] However, recently reported double network elastomers can exhibit extremely high mechanical strength of 60 MPa[2] and reach elongation at breakage as high as 3,300%.[3] To date, these dramatic enhancements have only been realized in water-based systems, limiting their utility in Army applications due to poor environmental stability. To realize the full potential of the double network concept for military application, we have been working toward preparing nonaqueous double-network gels. The primary challenge of developing double networks is their high level of complexity. There are a number of factors that determine the properties of simple polymer networks, including cross-linking chemistry, chain interactions, stiffness of the monomers, and cross-linking junctions; the presence of branching points, loop defects, and dangling chain ends; and the density of entanglements (Fig. 1). For double networks, these factors must be considered for each individual network as well as the interplay between each network. This complex dynamic presented substantial design challenges for preparing double networks for Army applications. In addition, double networks are difficult to process in a practical sense. Typically, the first network, which consists of a brittle, highly cross-linked network, is mixed and cured. This network is then backfilled with the precursors to the second

network, which forms a loosely cross-linked, highly elastomeric network, and cured a second time. Ideally, both networks would be formed in a single step while avoiding intercross-linking between networks and phase separation. Given the high level of complexity and difficulties in processing double networks, our approach was based on combining computationally aided materials design with experimentally driven formulation and characterization to streamline the process of identifying the critical variables that determine the mechanical performance of the networks.

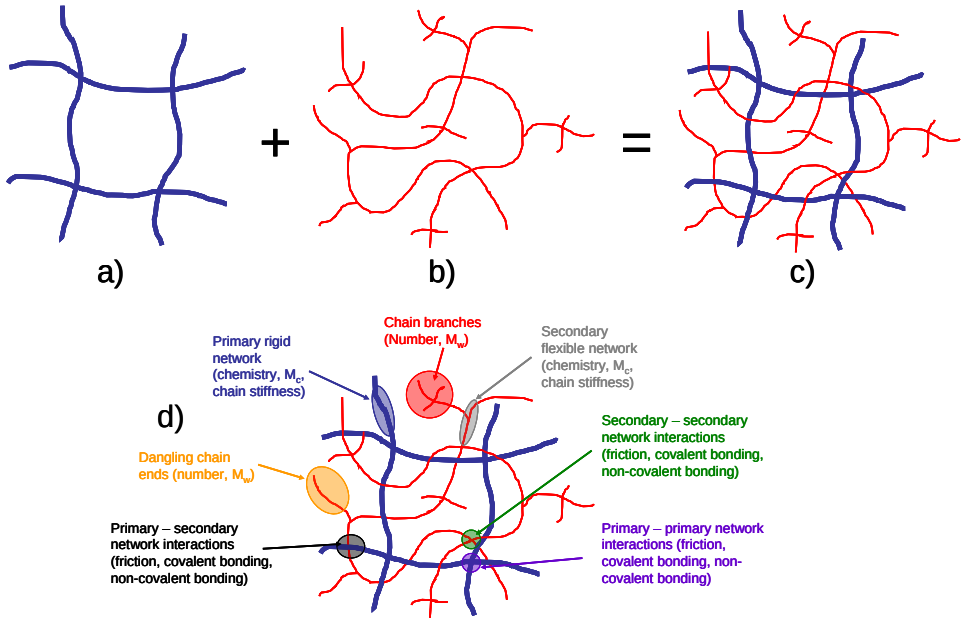

Fig. 1 A double network polymer is a molecular composite composed of a) a rigid primary network, combined with b) a more flexible secondary network to form c) a hybrid double network composed of the intertwined rigid and soft network. Also displayed is d) a schematic of the various interactions and chain architecture effects that must be included to describe the mechanical properties, toughness, and damping behavior of a double network over a broad range of temperature and frequency.

3. Results

3.1 Coarse-Grained Modeling of Polymer Gels with Rigid Side Chains

Formulating double networks is a cumbersome process that involves multiple curing and infiltration steps. Ideally, the double network would be formed in a single step to ensure practical application. We have developed a novel simulation scheme to investigate a potential route to preparing double networks in a single step. Here, we consider polymer melts composed of 50% of a chemically end-linked polymer network that is diluted in a thermal branched polymer solvent. All

solvent chains are composed of a flexible backbone of fixed length and rigid side chains or "spikes," where an angle between a trio of monomers is nearly 180°. We consider several polymer systems that differ in molecular architectures of polymer solvents, such as a structure of the branch point (2 long or 4 short spikes with the same total number of the rigid monomers) and distribution of the branched points (multiple or just 2 branch points at the ends of the chain). Linear polymer solvents of small and high molecular weight are also studied as reference systems.

The standard polymer coarse-grained, bead-spring Kremer-Grest model[4] was used to model the network curing process. This method has proved to be an excellent technique to the study the microscopic topology and dynamics of a wide variety of polymer networks and gels.[5–8] The pair interaction between topologically nonconnected particles is described by the standard truncated Lennard-Jones pair potential

$$U_{LJ}(r) = 4U_0\left[\left(\frac{a}{r}\right)^{12} - \left(\frac{a}{r}\right)^{6} - \left(\frac{a}{r_c}\right)^{12} + \left(\frac{a}{r_c}\right)^{6}\right], \quad (1)$$

where U_0 is the depth of the potential well, r_c is the cutoff distance, and a is the distance where the interparticle force is zero. We set $r_c = 2^{1/6}a$, yielding the so-called Weeks-Chandler-Andersen excluded volume potential, U_{WCA}. All quantities are expressed in terms of the mass m, intermonomer binding energy U_0, monomer diameter a, and characteristic time $\tau_{LJ} = \sqrt{ma^2/U_0}$.

Topologically bound monomers interact according to the standard finite extensible nonlinear elastic (FENE) potential / Lennard-Jones bonded potential, $U_{FENE/LJ}$, where $U_{FENE/LJ}(r) = U_{FENE}(r) + U_{WCA}(r)$. U_{FENE} is given by

$$U_{FENE}(r) = -\frac{a_{FENE}}{2}R_0^2 \ln\left[1 - \left(\frac{r}{R_0}\right)^2\right]. \quad (2)$$

The standard parameter values of the spring constant, $a_{FENE} = 30U_0/a^2$, and the maximum extension, $R_0 = 1.5a$, are used. Flexibility of the polymer chains is controlled through an angle-bending potential

$$U_a(\theta) = k(\theta - \theta_0)^2, \quad (3)$$

where θ is the angle between triplets of connected beads, $\theta_0 = \pi$ is the equilibrium value of the angle, and $k = 300U_0/\text{rad}^2$.

The precursor melt was equilibrated by our fast equilibration protocol,[9] and the end-linked polymer network was prepared by curing the linear chains and

tetrafunctional cross-linkers. The relaxation modulus in simple extension is evaluated from a stress-relaxation simulation, which consists of a volume-conserving elongation of the sample, followed by a long relaxation. Also, we performed a series of simulations of uniaxial tensile deformation at strain rates ranging from $\dot{e} = 2.5 \cdot 10^{-7}$ to $10^{-4} \tau_{LJ}^{-1}$. The elongational stress, σ in the system, is calculated from the normal pressure differences.

Figure 2a shows the relaxation tensile modulus, $E(t)$, at an engineering strain, ε, equal to 2.8. The value of ε is chosen to be below the onset of strain hardening; the stress response for smaller strains is small and difficult to determine from the noise. Although the solvent entanglements dominate the time-dependent response of polymer gels with the linear high-molecular-weight solvent at short times, $E(t)$ develops a plateau value similar to the polymer gel with low-molecular-weight solvent, which is dominated by the network structure composed of chemical cross-links and trapped physical entanglements. Our results indicate that rigid spikes aggregate in clusters to reduce the entropy penalty of the flexible polymer chains. While the short spikes exhibit the onset of this aggregation, the long spikes create an additional stable network (second network). As a result, $E(t)$ of the networks containing branched solvent with long spikes stays nearly constant, forming an equilibrium zone for a broad range of time. The long spike aggregation also contributes significantly to the tensile behavior, where the H- and comb- polymers with long spikes have a considerably higher stress response than the other branched polymers (Fig. 2b). This work demonstrates a potential experimental strategy toward preparing double networks in a single step. The full details of this work can be found in a recent publication.[10]

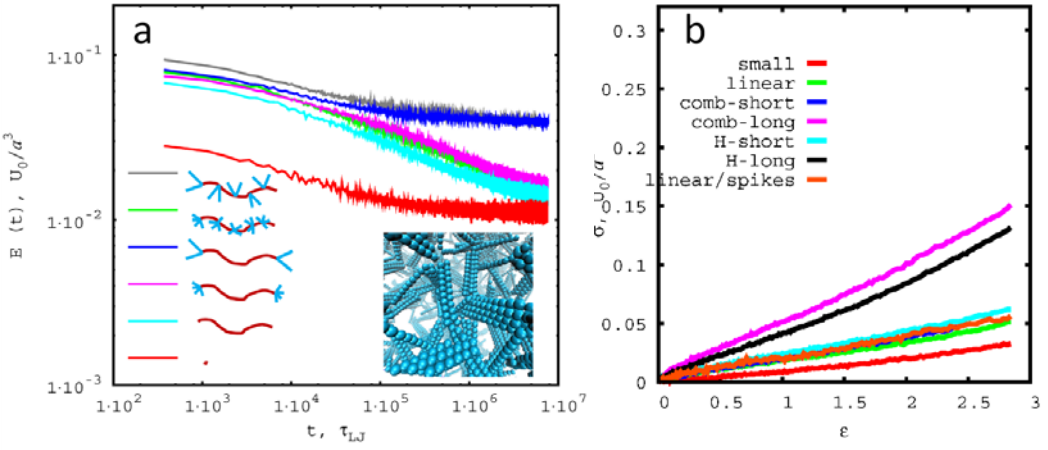

Fig. 2 a) Relaxation tensile modulus, $E(t)$, plotted against time for networks with different architectures of the solvent chains. The inlet shows aggregation of the long rigid spikes. b) True stress, σ, vs. engineering strain, ε.

3.2 Formulation of Rigid Epoxy Single Network Gels

Double networks consist of 2 intimately mixed networks absent any phase separation. Double networks are typically prepared by mixing and curing the first network followed by backfilling and curing the second network. We envisioned our first network consisting of a solvent swollen rigid epoxy gel based on curing diglycidal ether of bisphenol A (DGEBA) of various chain lengths with amine functionalized chains of poly(propylene glycol) (PPG) of different molecular weights in the presence of dibutyl phthalate at various solvent loadings (Fig. 3).

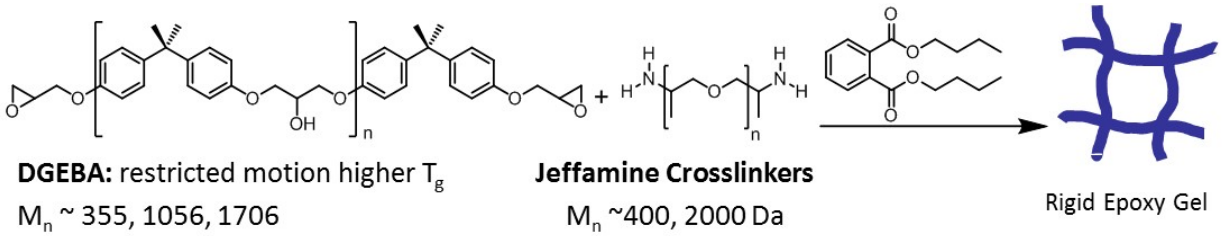

Fig. 3 Precursors used to form rigid epoxy single network gels

As mentioned previously, the resulting mechanical response of the single/double networks is affected by a number of factors. Variation of the chain length and rigidity of the polymer precursors and the presence of solvent can have a significant effect on the chain structure of gels due to formation of network defects, such as loops or dangling chain ends. In an effort to understand how the nature of the polymer precursors effects the network structure and mechanical behavior of the gels, a series of gels was prepared. Rheological measurements were performed to evaluate the mechanical response of the polymers in a temperature range of –100 to 100 °C. For each molecular weight precursor, the plateau modulus decreased with increasing solvent loading, and the peak in the tan δ curve shifts to lower temperature, indicating a decrease in the glass transition temperature (T_g) with increased solvent loading. The plateau modulus changes minimally with increasing molecular weight of the epoxy precursor (Fig. 4).

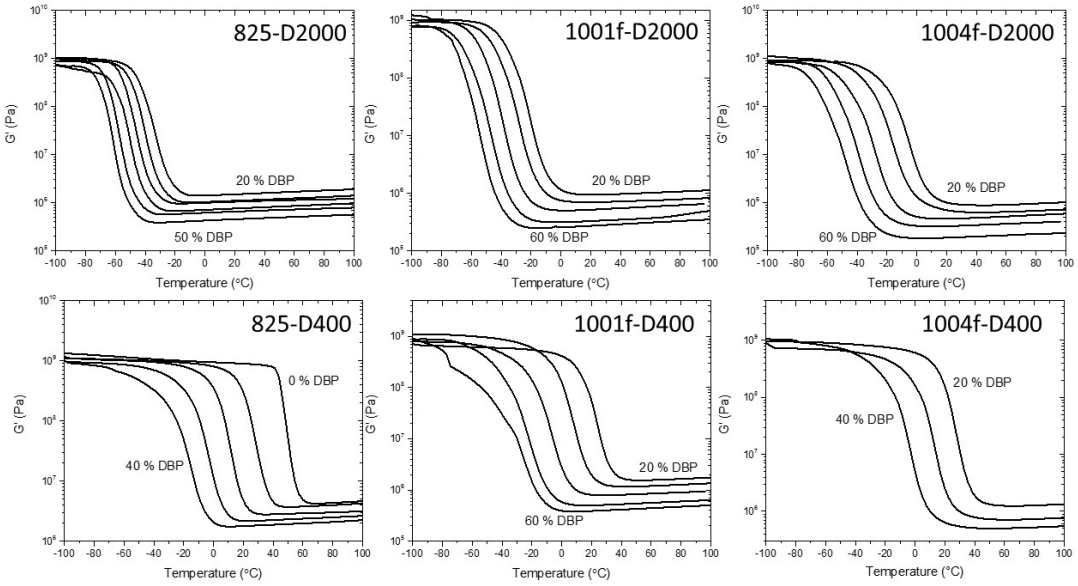

Fig. 4 Shear storage modulus as a function of temperature for DGEBA resins Epon 825, 1001f, and 1004f cured with amine curatives D400 and D200 in the presence of DBP

The log–log plots of the storage modulus in the plateau region (measured at T_g + 70 °C) as a function of polymer content in the gels are consistent with a linear fit, indicating power law behavior that can be described by the scaling factor taken from the slope of the linear fit (Fig. 5). For gels produced with the diamine precursor D400, the scaling factor increases from 1.77 to 3.13 as the molecular weight of the epoxy precursor increases. For gels produced with diamine precursor D2000, the change in scaling factor is less pronounced, increasing from 1.75 to 2.20. In both cases, as the molecular weight of the epoxy precursor increases, the presence of solvent has a greater impact on the network structure. The influence of solvent present during the curing process on the network structure and mechanical behavior is likely the result of loop defects that are formed. Loop defects result in network junctions not being elastically active, effectively reducing the shear storage modulus. Loop defects occur when a reactive chain end "back-bites" and bonds with another reactive group on the same chain. For our work, loop formation increases with increasing molecular weight of the epoxy precursor. We reason the increase in scaling factor with increasing molecular weight of the epoxy precursor is related to the stiffness of the precursor. For the Epon 825 precursor, the chain length is one monomer unit. Given the rigidity of the DGEBA unit, the likelihood of a back-biting reaction on the same polymer chain occurring, resulting in loop formation, is low. As the length of the DGEBA polymer chain increases, the chain can explore more conformations, increasing the likelihood of loop formation and resulting in a network junction that is not elastically active. Loop formation is enhanced with increasing solvent content as the local concentration of unreacted

amine groups along the polymer backbone in the vicinity of the unreacted epoxy chain end increases relative to the bulk concentration of unreactive amines in the reaction mixture. This work demonstrates the importance of considering not only the direct influence of polymer structure (chain length, stiffness) on mechanical performance but also how the polymer structure influences the cure process itself and the resulting network structure (chain junctions, loop defects, dangling chain ends).

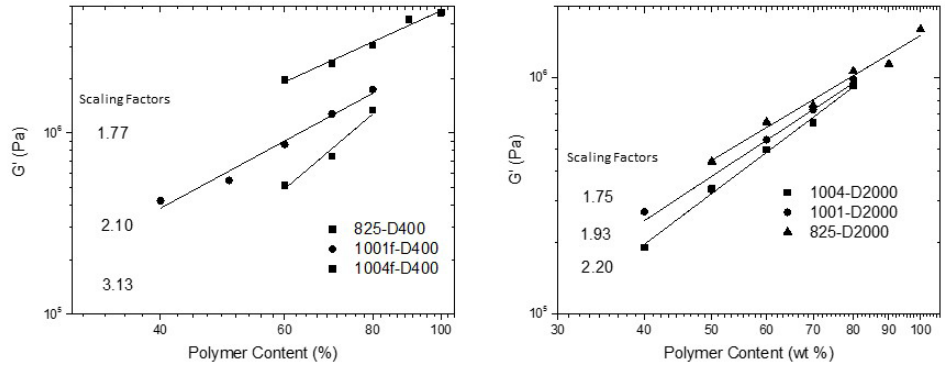

Fig. 5 Plot of shear storage as a function of polymer content using different epoxy/amine/solvent combinations involving DGEBA resins Epon 825, 1001f, and 1004f, and amine curatives D400 and D2000 cured in the presence of dibutyl phthlate. The lines represent a best fit for the data with scaling factors taken from the slope of the line.

3.3 Coarse-Grained Modeling of Epoxy Gels

To further understand the influence of chain structure on network structure during curing, we analyzed course-grained models of various polymer gels. Again, a standard course-grained, bead-spring Kremer-Grest model was used, similar to what was described previously. In this study, we considered a polymer gel, where the chemically end-linked polymer network is diluted in an athermal solvent. The total number of coarse-grained particles in all of our simulations is N_{tot} = 255,000–366,000, and the monomer number density is set to the conventional value of $\rho = 0.85\ a^{-3}$. All particles used to describe the polymer solvent and network interactions are described by the same excluded volume potential. The precursor melt is composed of the network precursor chains, tetra-functional cross-linkers, and solvent. All tetra-functional cross-linkers are flexible, while the precursor chains could either be flexible or semi-flexible. Rigidity in the precursor chains is enforced through the bending potential described in Eq. 3, where k_θ is $2.0Uo$ and $0.0Uo$ for semi-flexible and flexible chains, respectively. In this study, the effect of the length of the cross-linkers and precursor chains is considered, in addition to the rigidity of the precursor chains for a system composed of 80% polymer and 20% solvent. The systems that were considered for this polymer concentration are summarized in Table 1.

Table 1 Content of the simulated polymer gels of 80% of polymer content

System	Cross-linker length, beads	Precursor chains length, beads	Precursor chains rigidity
1	56	6	Flexible
2	56	6	Semi-flexible
3	56	20	Flexible
4	56	20	Semi-flexible
5	204	6	Flexible
6	204	6	Semi-flexible
7	204	20	Flexible
8	204	20	Semi-flexible

For brevity, the gel systems described in Table 1 will be referred by the prescribed system numbers for the remainder of the report. For system 5, we will also consider the effects of varying the polymer concentration from 10% to 100%.

The precursor melts were equilibrated by the fast equilibration protocol,[9] which has been shown to produce well-equilibrated entangled polymer melts. This method entails generating random configurations of polymer chains whose structures are as close as possible to equilibrated structures at large length scales. The chains are also initially allowed to pass through each other to accelerate the polymer dynamics by using a soft potential for nonbonded particles. A detailed description of this method can be found elsewhere.[9]

The end-linked network is dynamically formed during a constant particle, volume, temperature simulation in the presence of polymer solvent. Temperature is set to 1.0 U_0/k_B and is controlled during the entire simulation by a Langevin thermostat with a damping time of 1.0 τ_{LJ}. The molecular dynamics (MD) time step is $\Delta t = 0.01$ τ_{LJ}. The end particles of the cross-linkers and precursor chain react, resulting in a network structure connected by FENE bonds, which are formed when the distance between ends of a cross-linker and a linear precursor chain is less than 1.2a. To increase the curing rate, attractive Lennard-Jones (LJ) interactions ($r_c = 2.5a$) are included between end particles of the cross-linkers and precursor chains. The simulation is allowed to run until at least 96% of all possible bonds are formed. All simulations were executed using the Large-scale Atomic/Molecular Massively Parallel Simulator (LAMMPS).[11,12]

The structure of the polymer networks was analyzed, and the ratio of the different strand conformation was computed. When the precursor chain reacts, it can form either a network strand, loop, or dangling end. Unreacted precursors exist as free chains in the solution. A dangling end develops when only one end of a precursor chain reacts with the cross-link. If 2 ends of a precursor chain are attached to 2 different cross-linkers, then a network strand is formed. In contrast, if 2 ends of the

precursor are attached to the same cross-linkers, a loop is created. Loops formed from 2 reactive ends belonging to the same branching point are referred to as short loops, while loops formed from 2 different branching points that belong to the same cross-linker are labeled long loops. The schematic of the network structure is shown in Fig 6.

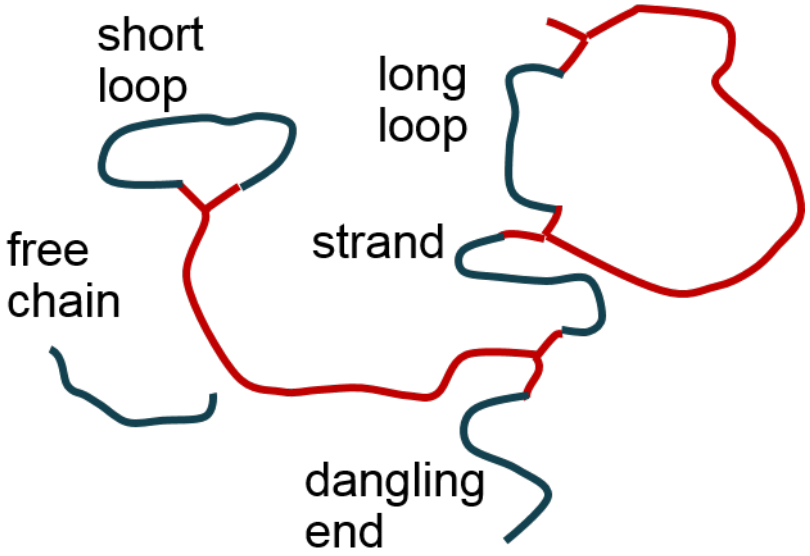

Fig. 6 Schematic representation of the network structure. The cross-linkers and chains are shown in red and blue, respectively.

Results of the network structure analysis are given in Table 2. Our results demonstrate that formation of loops at constant polymer loading is promoted by long cross-linkers, flexible monomers, and short monomers. If all these factors are concurrently present in the prepolymer mixture, as in the case of the system 5, the amount of loop defects becomes significant and the mechanical properties of these gels are expected to be inferior. The ratio associated with long loops is not very significant for all of the systems considered, although it is larger for systems that contain the shorter cross-linker, as expected. In addition, the results demonstrate that increasing the monomer length and rigidity reduces the number of loops even for cases that contained the long cross-linker (system 8).

Table 2 Percent content of strands, short and long loops, dangling ends, and free chain in the polymer gels. The cure is recorded as well.

System	Strands (%)	Short loops (%)	Long loops (%)	Dangling ends (%)	Free chains (%)	Cure (%)
1	89.57	6.58	1.32	2.53	0	98.73
2	91.45	4.95	1.47	2.13	0	98.93
3	93.58	2.77	1.35	2.28	0.02	98.84
4	94.18	1.95	0.78	3.03	0.05	98.43
5	75.58	20.58	0.46	3.38	0	98.31
6	80.54	15.33	0.88	3.25	0	98.38
7	87.79	7.79	0.75	3.63	0.04	98.15
8	93.08	3.17	0.71	3.00	0.04	98.46

The long cross-linker promotes the creation of loops by effectively decreasing the number of reactive ends. A similar effect occurs when the concentration of the polymer is decreased. For system 5, we performed additional simulations, where the polymer concentration was varied from 10% to 100%. As shown in Fig. 7, the loop concentration is reduced with increasing polymer concentration.

Further details of the experimental and computation results described above will be shared in a forthcoming publication currently in preparation.

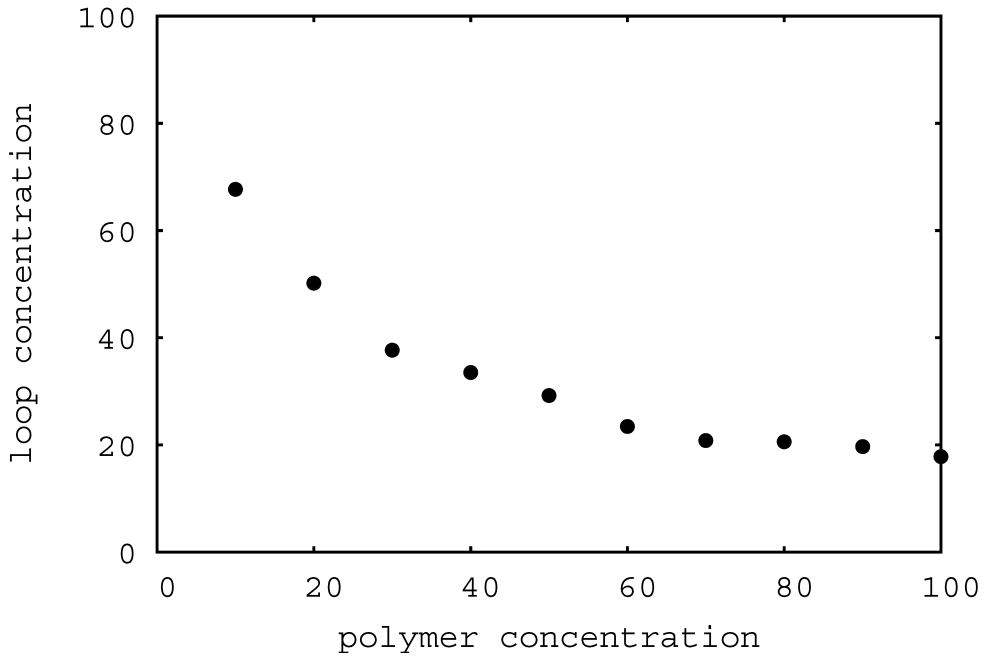

Fig. 7 Loop concentration as a function of the polymer concentration for system 5

3.4 Molecular Dynamics Simulations of Double Network Polymers

As mentioned previously, double network polymers are highly complex systems covering a broad parameter space since variables from each individual network must be considered in addition to how the 2 networks interact. Computational modeling can be used to elucidate and predict the mechanical properties of double networks over a broad parameter space, which is challenging to explore solely through experiments. In this work, we implemented a coarse-grained simulation technique to understand and predict the mechanical properties of a double network, where the first network is more tightly cross-linked than the second network. The effects of cross-linked density, the ratio of the highly to loosely cross-linked network, and the network interactions on the molecular level fracture toughness and the elastic modulus are presented.

MD simulations were performed as above using the Kremer-Grest bead-spring model. In this model, all monomers have a mass *m* and the pair interaction between topologically nonconnected monomers is described by the standard truncated LJ pair potential as described above. The LJ potential cutoff was chosen to be r_c = 2.5 *a*. The factor *n* is used to scale the interactions between the different monomers. For the interaction between monomers that makes up the first and second network, we consider 2 scenarios: an attractive interaction (*n* = 2.0) and a neutral interaction (*n* = 1.0); *n* is equal to unity for self-interactions among the monomers of first network and between monomers of second network. All quantities are expressed in terms of the inter-monomer binding energy U_0, monomer diameter *a*, and characteristic time $\tau_{LJ} = \sqrt{ma^2/U_0}$.

Topologically bound monomers interact through the sum of the purely repulsive LJ potential ($r_c = 2^{1/6}a$) or so-called Weeks-Chandler-Andersen U_{WCA} and a quartic potential U_q.[13,14] The quartic potential

$$U_q(r) = (r - \Delta r - b_1)(r - \Delta r - b_2)(r - \Delta r)^2 + U_0 \tag{4}$$

allows for bond breaking and prevents unbroken chains from crossing. This potential has a smooth cutoff at $r = \Delta r$, which preserves force continuity, where the potential parameters are $k = 1434.3\,u_0/a^4$, $b_1 = -0.7589a$, $b_2 = 0.0$, $\Delta r = 1.5a$, and $U_0 = 67.2234\,u_0$.[13] The parameters in $U_q(r)$ were obtained by fitting the bond force with the FENE potential at the first zero and the minimum. The ratio between the forces at which covalent and noncovalent bonds break, about 590, is a reasonable approximation for a coarse-grained polymer model,[13] and the model has been used

recently to study fractur.[13,15,16] Broken bonds are not allowed to reform in our simulations.

In the double network systems considered in this study, the first polymer network is tetra-functional and the second network is randomly cross-linked. The simulations are initiated by producing well-equilibrated, uncross-linked polymer melts. Periodic boundary conditions are applied along all 3 directions of the initially cubic simulation cells. A detailed description of the equilibration algorithm employed in this study is published elsewhere.[14] A schematic representation of these uncross-linked melts is provided in Fig. 8. After equilibrating the uncross-linked melts, we created the double network in 2 subsequent steps to exclude the phase separation. In the first step, the first network was cured in the presence of the monomers of the second network. After the first network finished curing, the second network was created. Single network systems containing either the first network or the second network were also built.

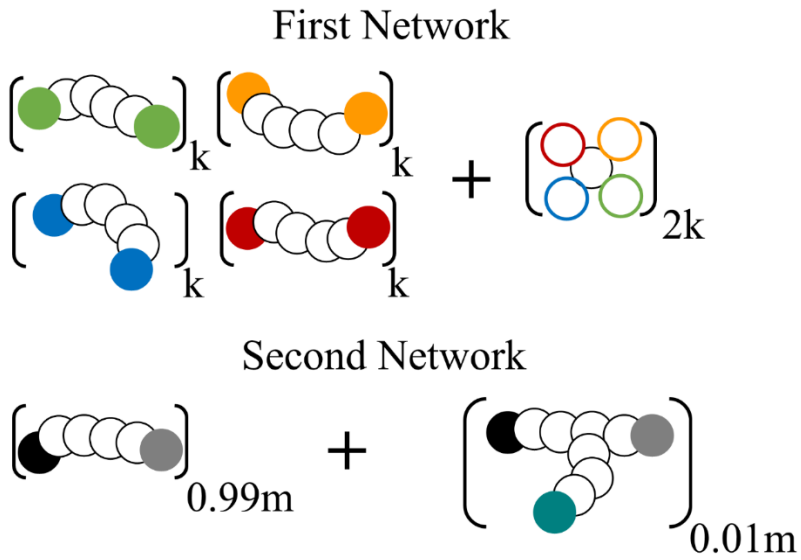

Fig. 8 Schematic representation of reactive polymer melt. To exclude loop defects, the end beads of the linear precursor chains (filled circles) of the first network react with the end beads of the cross-linkers of the same color (unfilled circles). The second network monomers were polymerized by reaction of the end beads of the same color, where loops are also excluded. The second network is then loosely cross-linked by reacting the 2 blue-green beads (filled circles) located at the end of the side chains.

In this work, we considered 2 volume fractions of the first network in the double network: 0.1 and 0.25. Two sizes of the linear precursor chains composing the first network, N_1, are also studied: N_1 = 6 and N_1 = 25 beads, along with 2 different attraction coefficients between the 2 networks, n = 1 and 2. We also consider systems composed solely of the first or second network. The total number of coarse-grained particles in our simulations, N_{tot}, is from 264,000 to 340,000. The 11

systems that were considered in this study are summarized in Table 3. The systems considered will be referred to by number for brevity.

Table 3 Content of the simulated polymer double network. Self-attraction coefficient between particles within a network (first or second) is fixed at 1.

System	Number of particles in the precursor chain in the first network	Volume fraction of the first network	Attraction coefficient between networks, *n*
1	6	0.1	1
2	6	0.25	1
3	6	0.1	2
4	6	0.25	2
5	25	0.1	1
6	25	0.25	1
7	25	0.1	2
8	25	0.25	2
9	6	1.0	NA
10	25	1.0	NA
11	0	0.0	NA

After preparing the networks, we performed a series of tensile deformation simulations at the constant true strain rate of $\dot{e} = 10^{-5}\tau_{LJ}^{-1}$. The employed strain rate is much higher than typical experimental strain rates and corresponds to ballistic impacts. We find, however, that it is still sufficiently slow, that segmental contributions to stress are small, and stress-strain curves match the predictions of linear and nonlinear rubber elasticity. A Langevin thermostat with damping time 1.0 τ_{LJ} is used to maintain T = 1.0, and a Nose-Hoover barostat with damping time 100 τ_{LJ} is used to maintain zero pressure along the transverse directions. All simulations were performed using LAMMPS.[11,12]

3.4.1 Mechanical Properties

The dense system of cross-links in polymer networks makes them very strong, but brittle and loosely cross-linked networks are generally ductile but have low modulus. Thus, there is significant research to determine methods to increase their toughness. One such method is through the use of the double network structure, which is composed from highly cross-linked first network and loosely cross-linked second network. Figure 9 shows our results for the double network, where the first network is very tightly cross-linked (N_1 = 6).

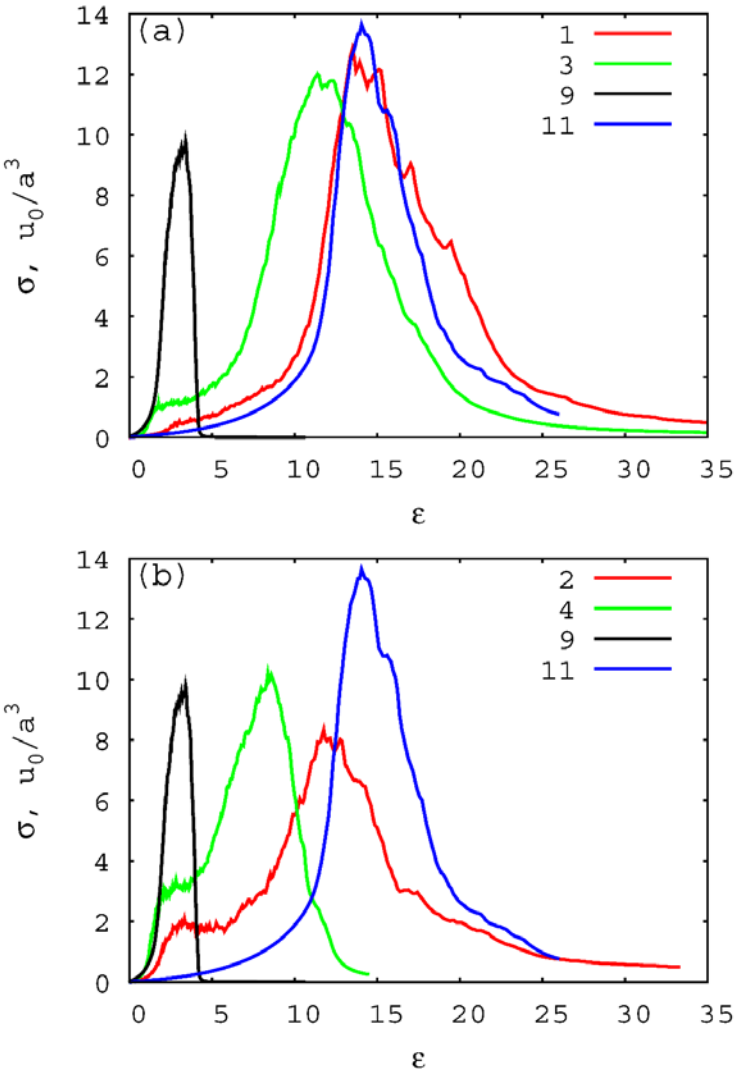

Fig. 9 True stress, *s*, vs. engineering strain, *e*, for the uniaxial tension for polymer networks for the very tightly cross-linked first network (N_1 = 6) and a ratio of the first and second networks, a) 1:9 and b) 1:3. The black and blue lines correspond to the single network composed of the first (system 9) and second networks (system 11), respectively.

Under deformation, the single network, which is composed of the strong first network, fails in a brittle fracture, breaking at low strain. On the other hand, the single network composed of the second network is capable of sustaining stress at a much higher elongation, but it has a much lower modulus (Fig. 9). When the volume fraction of the first network is 0.1 in the double network and there are no attractive interactions between the 2 networks (system 1), the elastic modulus and molecular-level fracture toughness of this double network are similar to values obtained for the single lightly cross-linked network (Fig. 9a). When an attractive interaction is added to the system (system 3), the elastic modulus becomes greater and the fracture toughness only slightly decreases. This increase in the elastic

modulus is related to the swelling of the first network strands, since the modulus in the infinitesimal deformation is given by $G_e = g(r_e^2 / r_0^2)\nu RT$, where g is a numerical factor that includes mobility contributions, ν is the concentration of network strands, R is the gas constant, and T is the temperature. The ratio r_e^2 / r_0^2 represents the amount of network swelling, where r_e^2 is the mean square end-to-end distance of a strand and r_0^2 is the mean square end-to-end distance of the same strand if not constrained by cross-links.

When the proportion of the first network in the double network is increased, so the ratio of the first network to the second network is 1:3, the double networks (systems 2 and 4) exhibit less ductile behavior (Fig. 9b). Although the elastic modulus of both double networks is closer to the first network and the elastic modulus of the system 4 (attractive interactions are present) is even greater than the modulus of the single first network, the molecular level fracture toughness decreases. Therefore, system 3 exhibits the most promising behavior.

When the first network is less cross-linked ($N_1 = 25$), our findings demonstrate that when the quantity for the second network (loosely cross-linked) dominates (the networks ratio is 1:9), the elastic modulus is only slightly influenced by the cross-link density of the first network (highly cross-linked), and the molecular level fracture toughness does not exhibit a significant dependence on it as shown in Fig. 10. For instance, systems 1 and 5 and systems 3 and 7 have very similar mechanical properties, with the exception that the modulus of system 3 is slightly higher than the modulus of system 7 (Figs. 9a and 10a).

When the quantity of the first network is more significant in the double network, where the ratio of the first network to the second network is 1:3, both the elastic modulus and the molecular-level fracture toughness are strongly dependent on the cross-link density of the first network (Figs. 9b and 10b). The elastic modulus decreases with decreasing cross-linking density of the first network (i.e., an increase in the strand length of the first network from 6 to 25 beads). On the contrary, the strength of the double networks increases as the cross-link density decreases, especially for systems where the attractive interactions between the 2 networks are absent. For instance, the strength of system 6 is high compared to system 2. Both systems have the same ratio of the first network to the second network (1:3) and no attractive interactions, but system 6 has a lower cross-link density than the first network (Figs. 9b and 10b).

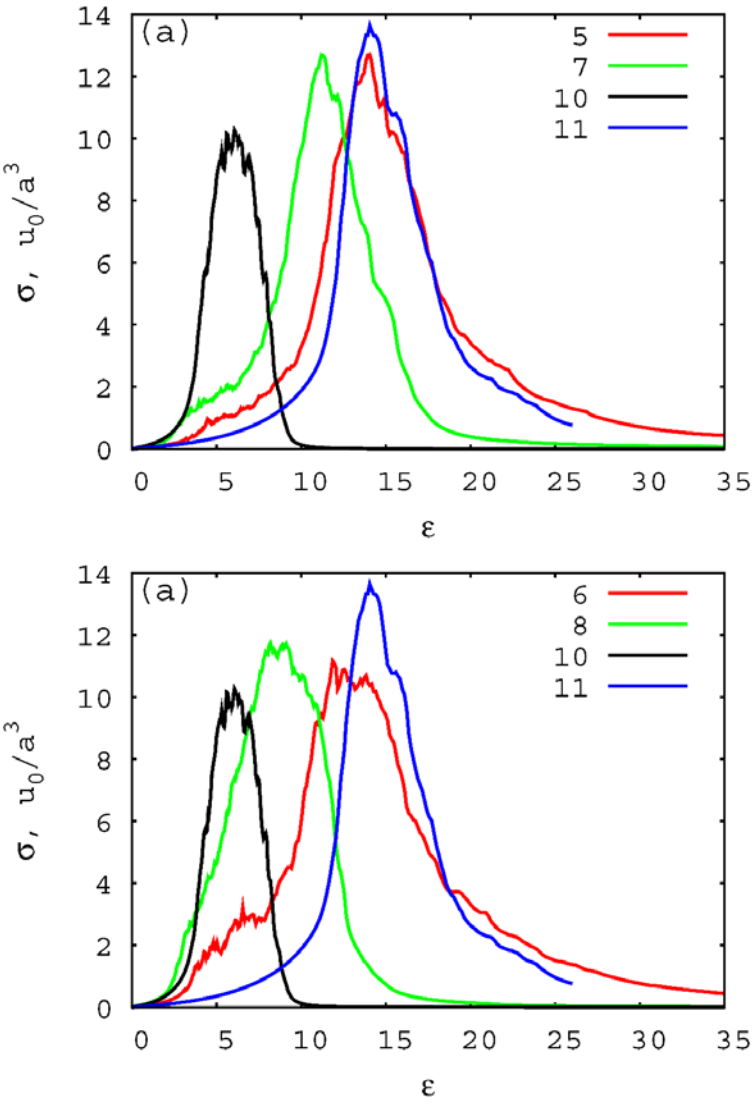

Fig. 10 True stress, *s*, vs. engineering strain, *e*, for the uniaxial tension for polymer networks for less tightly cross-linked first network (N_1 = 25) and a ratio of the first and second networks, a) 1:9 and b) 1:3. The black and blue lines correspond to the single network composed of the first (system 10) and second networks (system 11), respectively.

Taking these findings into account, we found that the 2 networks should have an attractive interaction and that the quantity of the first highly cross-linked network should be much less than the quantity of the second network, as in the case of system 3. Further details of this work can be found in a forthcoming publication.

3.5 Formulation and Characterization of Double Network Gels

Preparation of double networks involves curing one network in a first step followed by infiltrating that network with the reactive monomers that form the second network. The second network is then cured when the first network is fully swollen with the reactive monomers. This process is tedious but ensures intimate mixing of the 2 networks. Our simulations indicated optimal mechanical performance would be achieved if the ratio of the first network to the second network was low and if there was an attractive interaction between the 2 networks. Thus, we chose a system where the first network would become highly swollen in the second network to achieve a low ratio of first network to second network.

The first network consisted of a difunctional epoxy-functionalized PPG with a molecular weight of 640 cured with a difunctional amine-functionalized PPG with a molecular weight of 4,000. The cured network was backfilled with a solution of n-butyl acrylate containing a difunctional acrylate-functionalized polyethylene glycol with a molecular weight of 200 and a photo initiator (Irgacure 651) (Fig. 11).

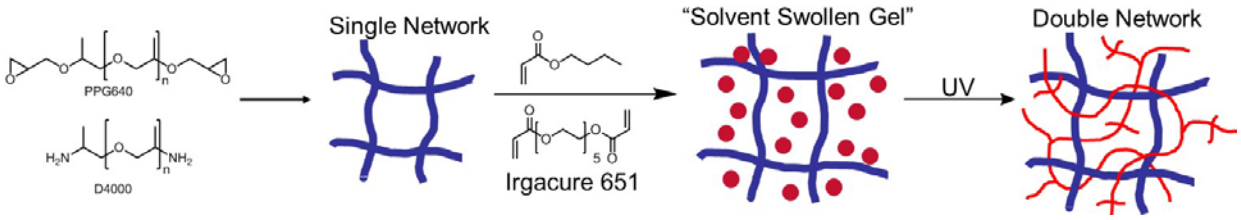

Fig. 11 Scheme for preparation of epoxy-acrylate double network

The epoxy network was allowed to swell in the n-butyl acrylate solution for 48 h before being cured under a UV lamp for 4 h. The final sample was 15 wt% epoxy network and 85% n-butyl acrylate, which is close to the ideal 1:9 first-to-second ratio of networks as identified in the simulations described previously. Rheological measurements were performed to evaluate the mechanical response of the networks in a temperature range of –130 to 100 °C (Fig. 12). The T_g of the epoxy single network is –55.19 °C, and the T_g of the butyl acrylate network is –37.53 °C. The T_g of the double network is –39.46 °C, which is very to close what is predicted using the Fox equation, –39.42 °C. This suggests the 2 networks are intimately mixed absent any phase separation.

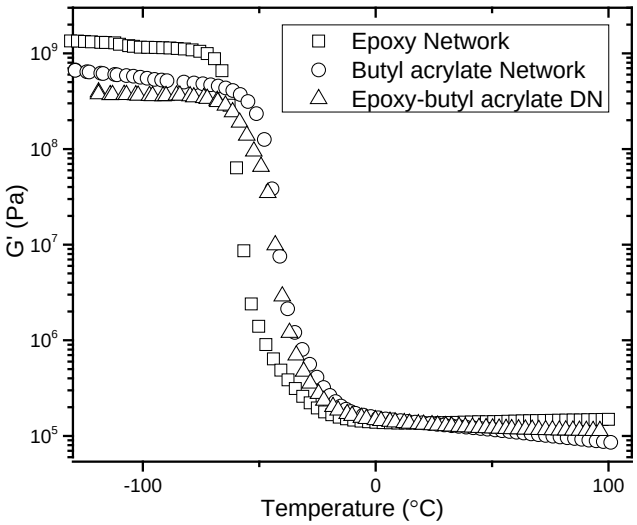

Fig. 12 Shear storage modulus as a function of temperature for the single and double networks

The single and double networks were also tested in tension using rectangular test specimens. The strain of the samples was measured by drawing a series of lines on the test specimens whose separation was tracked during the tensile test with a high-speed camera using the same frame rate as the load frame acquisition rate. The separation of the lines was measured from the images to determine the strain and correlated with the stress measurements. The results are shown in Fig. 13, where the performance of the double network was compared to the epoxy single network. Three epoxy single network specimens were tested and exhibited similar behavior, where at 150% strain the samples failed and exhibited a stress of 0.05 MPa. Because of difficulties in preparing defect-free double networks, only a single specimen was tested. Compared to the single epoxy networks, the double network supported significantly higher stress and higher strain. This initial test suggests the epoxy-acrylate double networks are significantly tougher than the epoxy single networks. However, additional stress-strain measurements and fracture toughness measurements are necessary to draw any definitive conclusions.

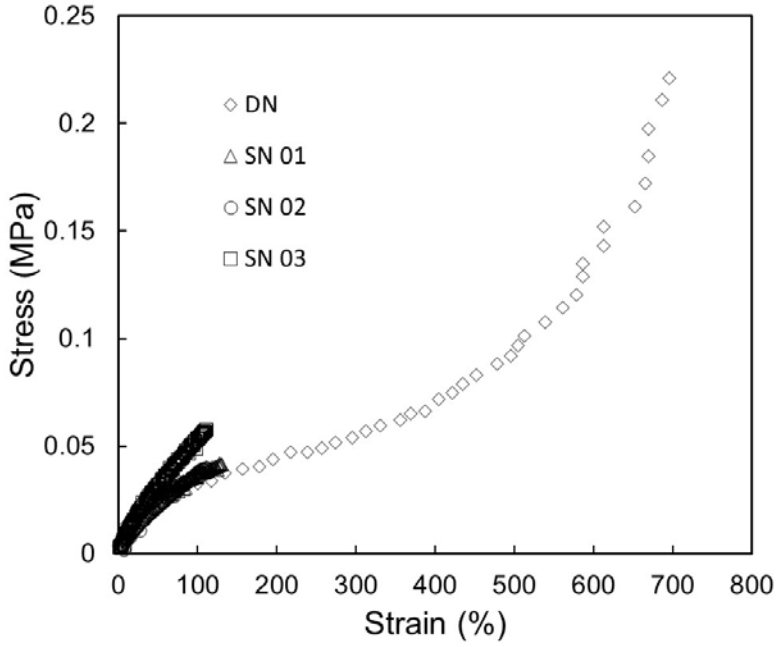

Fig. 13 Tensile deformation of epoxy single network and epoxy-butyl acrylate double network.

3.6 Development of Computational Tools for Coarse-Grained Modeling

A key component of this work involved developing new computational methods to more accurately capture the structure, chemistry, and mechanics of coarse-grained polymer models. Several significant advancements were made through this effort that enable more accurate descriptions of polymer behavior. These efforts and their implications are summarized in the following subsections.

3.6.1 Aggressive Coarse-Graining of Polymers

In the initial efforts of this Director's Research Initiative, several coarse-grained models were evaluated for the purpose of representing double networks. These include dissipative particle dynamics, a technique which represents polymers as a sequence of beads that interact using a soft interaction potential. Although such models capture the chain structure, the accuracy of their dynamics and mechanics suffers because of unphysical "crossing" of the polymer chains. A high-performance parallel code was developed that implements the modified segmental repulsive potential (mSRP) and segmental repulsive potentials (SRPs) to prevent crossing of the polymer chains.[17] This novel implementation is now packaged with the open-source MD engine LAMMPS and is available to the scientific community at large. Implementing these potentials into LAMMPS has made them more applicable and competitive with other coarse-grained models by dramatically improving their

computational performance. An example of the strong scaling behavior is given in Fig. 14; we have found excellent parallel performance up to the maximum number of CPU cores that were tested (512 cores, 375 atoms/core).

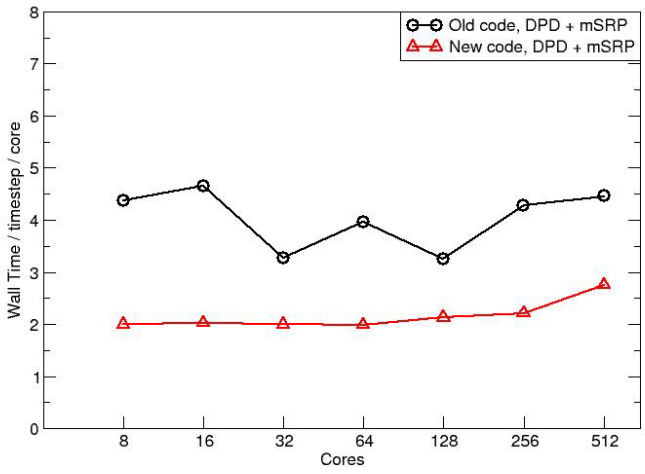

Fig. 14 Computational time required for dissipative particle dynamics + mSRP polymer chain model, normalized by time step and number of CPU cores

3.6.2 Sticky Bonds

Current MD codes lack functionality to capture transient "directional bonding" of polymer chains on the coarse-grained level, such has hydrogen bonds. We have extended LAMMPS to alter bond connectivity with Monte Carlo moves, during dynamics (hybrid MD–Monte Carlo). This feature is intended to capture the continuous breaking and reforming of transient bonds ("sticky bonds") that is expected to occur during high-strain tests. The current code is restricted to a simple Kremer-Grest potential for nonbond potentials and FENE bonds.

3.6.3 Polymer Network Builder

We developed an optimization scheme to construct unentangled polymer networks at the coarse-grained level without dynamics, using simulated annealing with Metropolis Monte Carlo. The network bond connectivity is optimized by assigning bonds between polymer chains such that the energy of the bonds is minimized. The optimization procedure begins with a randomly assigned solution of the chain connectivity (black bars); this solution is then improved by proposing different bond connections that are accepted or rejected with a probability (blue bars). After the system connectivity is optimized, the system undergoes a final relaxation (green bar) (Fig. 15).[18]

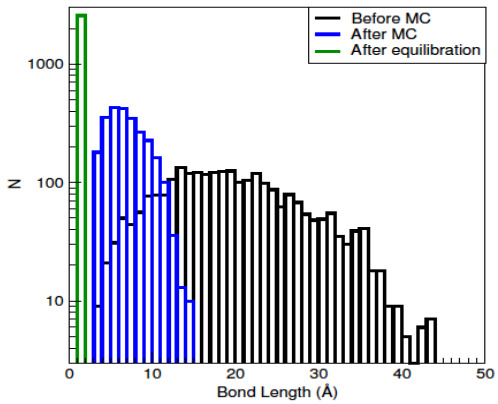

Fig. 15 Histogram of bond lengths during the optimization process. The bond length distribution is shown for a random starting condition (black), after Simulated Annealing (blue), and after equilibration (green).

4. Conclusion

The focus of this project was to develop novel, tough polymer networks and gels based off of a double network concept. Our approach was based on combing computationally aided materials design with experimental formulation and characterization. Computational efforts focused on developing coarse-grained MD simulations to predict the mechanical behaviors of several types of double networks. One such model identified a possible strategy for preparing double networks in a single step using polymer solvents bearing rigid branched chains. We also performed coarse-grained MD simulations of generic double networks, which showed that the elastic modulus and molecular-scale fracture toughness of double networks well above their T_g's depend on cross-linked density, the ratio of the highly to loosely cross-linked network, and the network interactions. Several new computational tools were also developed that enabled for more accurate descriptions of model polymer networks in MD simulations. Experimentally, epoxy-amine single network gels were formulated to determine how changing chain structure and solvent loading can affect network structure and mechanical behavior. Our results suggest that chain length and stiffness of the reactive precursors greatly impact the propensity for loop formations (network defects) in epoxy-amine gels, which significantly influences mechanical properties. An epoxy-butyl acrylate double network was also prepared. Preliminary tensile tests demonstrated significant enhancement in the elongation to break up the double network over the epoxy single network.

5. References

1. Matbase. Butadiene rubber [accessed 2016 Feb 9]. http://www.matbase.com/material/polymers/elastomers/butadiene-rubber/properties
2. Nakajima T, Furukawa H, Tanaka Y, Kurokawa T, Osada Y, Gong JP. Macromolecules. 2009;42:2184.
3. Tang Q, Sun X, Li Q, Wu J, Lin J. J Coll Interface Sci. 2009;339:45.
4. Kremer K, Grest G. J Phys Condens Matter. 1990;2:SA295–298.
5. Grest G, Pütz M, Everaers R, Kremer K. Non-cryst Solids. 2000;274:139.
6. Svaneborg C, Everaers R, Grest G, Curro J. Macromolecules. 2008;41:4920–4928.
7. Sliozberg Y, Chantawansri T. J Chem Phys. 2013;139:194904.
8. Sliozberg Y, Mrozek R, Schieber J, Kröger M, Lenhart J, Andzelm J. Polymer. 2013;54:2555–2564.
9. Sliozberg YR, Andzelm JW. Chem Phys Lett. 2012;523:139–143.
10. Sliozberg YR, Chantawansri TL, Lenhart JL, Andzelm JW. Polymer. 2014; 55:5266.
11. Plimpton S. J Comp Phys. 1995;117:1–19.
12. LAMMPS molecular dynamics simulator. Albuquerque (NM): Sandia National Laboratories; nd [accessed 2016 Feb 9]. http://lammps.sandia.gov.
13. Tsige M, Stevens MJ. Macromolecules. 2004;37(2):630–637.
14. Stevens MJ. Macromolecules. 2001;34(5):1411–1415.
15. Rottler J, Robbins MO. Phys Rev E. 2003;68:011801.
16. Mukherji D, Abrams CF. Phys Rev E. 2009;79:061802.
17. Chantawansri TL, Sirk TW, Sliozberg YR. J Chem Phys. 2013;138:024908.
18. Jang C, Sirk TW, Andzelm JW, Abrams CF. Macromol Theory Simul. 2015; 24:260.

List of Symbols, Abbreviations, and Acronyms

DGEBA	diglycidal ether of bisphenol A
FENE	finite extensible nonlinear elastic
LAMMPS	Large-scale Atomic/Molecular Massively Parallel Simulator
LJ	Lennard-Jones
MD	molecular dynamics
mSRP	modified segmental repulsive potential
PPG	poly(propylene glycol)
SRP	segmental repulsive potential
T_g	glass transition temperature

1 (PDF)	DEFENSE TECHNICAL INFORMATION CTR DTIC OCA
2 (PDF)	DIRECTOR US ARMY RESEARCH LAB RDRL CIO LL IMAL HRA MAIL & RECORDS MGMT
1 (PDF)	GOVT PRINTG OFC A MALHOTRA
4 (PDF)	DIR USARL RDRL WMM G R LAMBETH J LENHART T SIRK Y SLIOZBERG